If Anthropogenic CO_2 Emissions Cease, Will Atmospheric CO_2 Concentration Continue to Increase?

ANDREW H. MACDOUGALL, MICHAEL EBY, AND ANDREW J. WEAVER

School of Earth and Ocean Sciences, University of Victoria, British Columbia, Canada

(Manuscript received 18 October 2012, in final form 31 May 2013)

ABSTRACT

If anthropogenic CO_2 emissions were to suddenly cease, the evolution of the atmospheric CO_2 concentration would depend on the magnitude and sign of natural carbon sources and sinks. Experiments using Earth system models indicate that the overall carbon sinks dominate, such that upon the cessation of anthropogenic emissions, atmospheric CO_2 levels decrease over time. However, these models have typically neglected the permafrost carbon pool, which has the potential to introduce an additional terrestrial source of carbon to the atmosphere. Here, the authors use the University of Victoria Earth System Climate Model (UVic ESCM), which has recently been expanded to include permafrost carbon stocks and exchanges with the atmosphere. In a scenario of zeroed CO_2 and sulfate aerosol emissions, whether the warming induced by specified constant concentrations of non-CO_2 greenhouse gases could slow the CO_2 decline following zero emissions or even reverse this trend and cause CO_2 to increase over time is assessed. It is found that a radiative forcing from non-CO_2 gases of approximately $0.6\,W\,m^{-2}$ results in a near balance of CO_2 emissions from the terrestrial biosphere and uptake of CO_2 by the oceans, resulting in near-constant atmospheric CO_2 concentrations for at least a century after emissions are eliminated. At higher values of non-CO_2 radiative forcing, CO_2 concentrations increase over time, regardless of when emissions cease during the twenty-first century. Given that the present-day radiative forcing from non-CO_2 greenhouse gases is about $0.95\,W\,m^{-2}$, the results suggest that if all CO_2 and aerosols emissions were eliminated without also decreasing non-CO_2 greenhouse gas emissions CO_2 levels would increase over time, resulting in a small increase in climate warming associated with this positive permafrost–carbon feedback.

1. Introduction

In the present climate approximately half of the carbon emitted to the atmosphere is taken up by the oceans and the terrestrial biosphere, greatly mitigating the effect of anthropogenic carbon emissions on climate (Denman et al. 2007). Whether these negative carbon cycle feedbacks will continue to operate into the future (e.g., Friedlingstein et al. 2006) or after the cessation of anthropogenic CO_2 emissions (e.g., Gillett et al. 2011) is a subject of recent scientific interest. There are five components of the global carbon cycle that act on centennial or shorter time scales that are important for conceptualizing the mass balance of the atmospheric carbon pool. These are 1) enhanced soil respiration, 2) CO_2 fertilization, 3) ecosystem changes, 4) uptake of carbon by the surface ocean, and 5) transport of carbon into the deep ocean.

Enhanced soil respiration occurs when an increase in soil temperature induces heterotrophic organisms to consume soil carbon at a faster rate and continues until the rate of plant litterfall into the soil matches the soil respiration rate (e.g., Jenkinson et al. 1991). Enhanced soil respiration is initiated as soon as soils come into thermal equilibrium with an increased surface temperature (Luo and Zhou 2006). In temperature and tropical climates this typically occurs within a year of the change in surface temperature, but in polar climates can be significantly delayed by latent heat effects in permafrost soils (Schuur et al. 2008).

Adding CO_2 to the atmosphere will promote plant growth via CO_2 fertilization (Denman et al. 2007), unless other nutrient limitations or environmental conditions are preventing increased growth. This effect begins as soon as atmospheric CO_2 concentration increases and ceases once plant growth comes into equilibrium with

Corresponding author address: Andrew H. MacDougall, School of Earth and Ocean Sciences, University of Victoria, 3800 Finnerty Road, Victoria BC V8W 3V6, Canada.
E-mail: ahmacd@uvic.ca

DOI: 10.1175/JCLI-D-12-00751.1

the new CO_2 concentration (Denman et al. 2007). At high atmospheric CO_2 concentrations (circa 800–1000 ppmv) CO_2 fertilization saturates since CO_2 concentration is no longer rate limiting for photosynthesis in C3 plant species (Falkowski et al. 2000).

Changes in climate can induce ecosystem changes as plant species migrate to climates that meet their physiological needs (e.g., Baldocchi and Valentini 2004). The transition from one ecosystem to another can be sudden, as in the case of the rain forest to grassland transition seen in some climate models (e.g., Malhi et al. 2009). In many manifestations, however, ecological transition occurs slowly as the result of the decennial time scale for tree growth (Baldocchi and Valentini 2004). Ecosystem changes can be either a positive or negative carbon cycle feedback depending on whether afforestation or deforestation is being induced. In tropical regions, increases in temperature are expected to inhibit plant growth by increasing water stress and exceeding plant physiological limits. At high latitudes, warming is expected to enhance plant growth by increasing the length of the growing season. Anthropogenic land use changes also induce positive or negative carbon cycle feedback though deforestation, agricultural practices, and the abandonment of formerly cultivated lands (Denman et al. 2007).

The ocean takes up and releases CO_2 as a function of the gradient in the partial pressure of CO_2 between the surface of the ocean and the atmosphere (Denman et al. 2007). If atmospheric CO_2 concentration is increased from nonoceanic sources (e.g., fossil fuel emissions or deforestation), the partial pressure difference between the surface ocean and the atmosphere increases. This creates a stronger partial pressure gradient and increases the rate of ocean uptake of CO_2 (Friedlingstein et al. 2006). The strength of this feedback is constrained by the temperature dependence of the solubility of CO_2 in water and by the carbonate chemistry of the ocean (e.g., Greenblatt and Sarmiento 2004). Like most other gases, the solubility of CO_2 in water decreases with an increase in water temperature, such that the partial pressure of CO_2 in water is higher at a higher temperature for the same aqueous concentration of CO_2 (e.g., Greenblatt and Sarmiento 2004). The carbonate buffering system of the ocean allows the oceans to hold far more carbon than would be possible in distilled water (Falkowski et al. 2000). When CO_2 dissolves in the ocean it quickly comes into equilibrium with other species of dissolved inorganic carbon:

$$CO_2 + CO_3^{2-} + H_2O \leftrightarrow 2HCO_3^- . \quad (1)$$

The surface ocean has a limited supply of the CO_3^{2-} anions so that as more inorganic carbon is added to the ocean, a higher fraction of the carbon will be held as $CO_{2(aq)}$, until such time that the ocean can dissolve more CO_3^{2-} from sediments (Le Qéré and Metzl 2004). Therefore, as the climate warms, due to increasing atmospheric CO_2, the relative fraction of the fossil carbon that the surface ocean is able to take up is reduced (Denman et al. 2007).

Carbon is exported from the surface ocean to the ocean interior though subduction of cold dense (CO_2 enriched) water at deep-water formation sites (in the North Atlantic and Southern Ocean) and via the biological pump (e.g., Sigman et al. 2010). The biological pump is the transport of organic carbon into the deep ocean from its production at the surface. In the ocean interior, this organic material is oxidized into CO_2 (Greenblatt and Sarmiento 2004). Changes in the meridional overturning circulation (MOC) and biological activity in the surface ocean affect this sink of carbon in the deep ocean (Denman et al. 2007).

In most models of the global carbon cycle, the carbon cycle feedbacks together have a stabilizing effect on climate. Higher CO_2 concentration induces warming and enhanced soil respiration but also increases plant growth and the ocean uptake of carbon. In models, the ocean and land vegetation generally absorb more carbon than soils are emitting (Friedlingstein et al. 2006).

Anthropogenically produced greenhouse gases besides CO_2 contribute to climate change (Forster et al. 2007). The most important of these well-mixed species are CH_4, N_2O, and halocarbons that respectively contributed radiative forcings of 0.48, 0.16, and 0.34 $W\,m^{-2}$ in 2005. The atmospheric lifetimes of CH_4 and N_2O are 12 and 114 years, respectively. The halocarbons have lifetimes ranging between decades and thousands of years (Forster et al. 2007). Non-CO_2 greenhouses gases interact with carbon cycle dynamics in that they contribute to the warming of the climate without inducing CO_2 fertilization or strengthening the gradient in CO_2 partial pressure between the atmosphere and the ocean (Huntingford et al. 2011). That is, these gases do not induce two of the powerful negative feedbacks to climate change while contributing to the enhanced soil respiration, reduction in the solubility of CO_2 in the ocean, as well as to temperature-induced ecosystem changes. In this manuscript, non-CO_2 greenhouse gas forcings are reported as anomalies from preindustrial non-CO_2 greenhouse gas forcing.

Sulfate aerosols reflect shortwave radiation back into space, producing a negative radiative forcing with respect to the planetary surface (Murphy et al. 2009). Throughout most of the industrial age, the net effect of the sulfate aerosols has roughly canceled out the positive radiative forcing from non-CO_2 greenhouse gases

(Forster et al. 2007; Murphy et al. 2009). The atmospheric lifetime of sulfate aerosols is on the order of days to weeks (Lohmann and Feichter 2005). Therefore, a constant source of these aerosols is needed to maintain their presence in the atmosphere. The largest source of sulfate aerosols to the atmosphere is fossil fuel burning (Forster et al. 2007). It is expected that if the anthropogenic burning of fossil fuels were to suddenly cease, then aerosols would rain out of the atmosphere shortly thereafter removing the negative radiative forcing they presently produce. The experiments detailed below contemplate the effects on the global carbon cycle of the complete cessation of anthropogenic carbon emissions on centennial time scales. We assume that the effects of sulfate aerosols dissipate within weeks of such an event and therefore assume that the radiative forcing from sulfate aerosols is zero after the cessation of carbon emissions. However, not all aerosol forcing is associated with fossil fuel emissions so it is not implausible that significant aerosol emissions from biomass burning and anthropogenic sources could continue after fossil fuel emissions cease.

Experiments using Earth system climate models have suggested that if anthropogenic carbon emissions were to cease that natural carbon sinks would continue to operate, slowly scrubbing CO_2 out of the atmosphere (Matthews and Weaver 2010; Gillett et al. 2011; Matthews and Zickfeld 2012). The inclusion of a permafrost carbon component into the University of Victoria (UVic) Earth System Climate Model (ESCM) has strengthened the soil respiration feedback, which modifies the response of the model to the immediate cessation of anthropogenic emissions (MacDougall et al. 2012). When forced with a constrained and prescribed climate sensitivity of 3.0°C, atmospheric CO_2 remains almost constant for centuries after the cessation of anthropogenic carbon emissions, no matter when carbon emissions cease in the twenty-first century (MacDougall et al. 2012). The model result that under specified conditions CO_2 remains constant in the atmosphere after the cessation of anthropogenic CO_2 emissions suggests that there is a magnitude of non-CO_2 greenhouse gas forcing that induces a balance between modeled carbon sources and sinks. Here, we develop a method to find this carbon cycle balance point, explore the consequences of exceeding this threshold, and discuss the circumstances of why this balance may be attainable in the natural world.

2. Methods

a. Model description

The UVic ESCM is a coupled climate model of intermediate complexity (Weaver et al. 2001) with fully coupled oceanic (Schmittner et al. 2008) and terrestrial carbon cycle components (Matthews et al. 2004; Meissner et al. 2003). For this study, the permafrost carbon version of the UVic ESCM is used. The frozen ground component of this model is described in Avis et al. (2011) and Avis (2012). The parameterization of the permafrost carbon pool is described in MacDougall et al. (2012).

The oceanic carbon cycle component of the UVic ESCM is composed of an Ocean Carbon Cycle Model Intercomparison Project–type inorganic carbon cycle model. The ocean biology is simulated using a nutrient–phytoplankton–zooplankton–detritus ecosystem model (Schmittner et al. 2008). An oxic-only model of sediment respiration is used to simulate ocean sedimentary processes (Archer 1996). Terrestrial vegetation is simulated using the Top-Down Representation of Interactive Foliage and Flora Including Dynamics (TRIFFID) dynamic vegetation model coupled to a simplified version of the Hadley Centre Met Office surface exchange scheme (Meissner et al. 2003). The subsurface scheme has been modified to a 14-layer representation, extending down to a depth of 250 m, with exponentially increasing layer thicknesses (Avis et al. 2011). The modified subsurface scheme allows for freeze–thaw processes and has spatially varying thermal and hydraulic properties. These properties are interpolated to the model grid from soil mineral properties and organic content from the International Satellite Land Surface Climatology Project soil database (Scholes and de Colstoun 2012).The soil contains two carbon pools: an active carbon pool and a permafrost carbon pool. The active carbon pool is generated by the balance of heterotrophic soil respiration and plant litterfall from the TRIFFID vegetation model. The permafrost carbon pool exists only in soil layers that have been permanently frozen since model spinup. The permafrost carbon is assigned a globally uniform carbon density. If a permafrost layer thaws, it (and the carbon within it) is irreversibly transferred to the control of the active soil carbon component. Thereafter, the carbon within the layer will begin to decay (MacDougall et al. 2012).

To allow atmospheric CO_2 to freely evolve, the UVic ESCM is forced with carbon emissions. Certain experiments detailed below are forced using emission pathways diagnosed from representative concentration pathways (RCPs). These diagnosed emissions pathways (DEPs) were derived by forcing the UVic ESCM with each RCP and diagnosing fossil fuel emissions as a residual of the global carbon cycle [see supplementary materials of MacDougall et al. (2012) for a detailed description and validation]. The UVic ESCM's inherent climate sensitivity of 3.2°C is used in all experiments.

b. Allowing for balance

In the Canadian Earth System Model (CanESM) and previous versions of the UVic ESCM, the immediate response to a complete cessation of anthropogenic carbon emissions is a fast drop in atmospheric CO_2 concentration that lasts for approximately 20 years (Matthews and Zickfeld 2012; Gillett et al. 2011). After the system has had time to adjust to the sudden cessation of anthropogenic emissions, atmospheric CO_2 goes into a slow exponential decline in these simulations. The ocean uptake and CO_2 emissions from the terrestrial biosphere cannot be balanced during these first 20 years with a plausible non-CO_2 greenhouse gas forcing (during this period in most experiments the terrestrial biosphere is transitioning from a sink to a source of carbon). However, after the system adjusts to the sudden change in forcing, it may be possible to induce a balance. For the remainder of this discussion we will focus on this period beyond the first 20 years after the cessation of anthropogenic emissions. The 20-yr period is likely a consequence of the abrupt cessation of anthropogenic emissions. A gradual elimination of emissions would presumable lead to a more continues transition to a post–fossil fuel global carbon cycle.

c. Finding balance

Here, we infer that for a given quantity of cumulative carbon emissions there is a magnitude of non-CO_2 greenhouse gas forcing that will induce a balance between terrestrial carbon emissions and the ocean uptake of carbon for the period starting 20 years after the cessation of anthropogenic carbon emissions. To find this magnitude of non-CO_2 greenhouse gases, an iterative root finding method is used:

(i) After the cessation of anthropogenic CO_2 emissions, the UVic ESCM is run for 100 years forced under a constant aggregated non-CO_2 greenhouse gas forcing (R_{agg}).
(ii) The earth system is allowed to adjust after the cessation of CO_2 emissions for 20 years.
(iii) If CO_2 accumulates in the atmosphere after the 20-yr adjustment period, the experiment is repeated with a reduced R_{agg}.
(iv) If instead CO_2 decreases in the atmosphere after the 20-yr adjustment period, the experiment is repeated with an increased R_{agg}.
(v) This loop is continued until atmospheric CO_2 is balanced to within 2.0 ppmv over the last 80 years of the simulation.

If a balance cannot be found then one or more of the assumptions that have been made must be false. See section 4a for a discussion of the conditions under which this method can work.

d. Experiments

Three balance experiments were conducted by varying the rate of anthropogenic carbon emissions. In all the experiments the iterative method was used to find the carbon balance point for cumulative anthropogenic emissions of 80, 160, 320, 640, 980, and 1920 Pg of carbon (Pg C). In the pulse experiment, carbon was emitted to the atmosphere over the course of 1 year. There were no sulfate aerosols or volcanic events in this experiment, and agricultural areas were held constant at their preindustrial extent. In the ramp-up experiment, carbon was increased at a rate of 1% of total emissions per year for 100 yr. During the 100-yr ramp-up, agricultural areas were held constant at a preindustrial extent; there were no sulfate aerosols, no volcanic events, and non-CO_2 greenhouse gas forcing was held at zero.

In the transient emissions experiment, emissions pathways were followed until the required amount of carbon had been released into the atmosphere. During the transient period, the prescribed non-CO_2 greenhouse gas, sulfate emissions, volcanic events, land-use changes, and solar output variation were followed for each DEP. When cumulative anthropogenic carbon emissions reached the desired total carbon, sulfate emissions were instantaneously reduced to zero. After the cessation of carbon emissions, agricultural areas were held constant, and volcanic events and the solar output were fixed to their long-term means. The DEPs 8.5, 6.0, and 4.5 were followed; although most of the cumulative emission integration points occur before the DEPs diverge (DEP 2.6 is set aside due to the negative anthropogenic emissions required under that pathway).

Additional experiments were conducted for magnitudes of non-CO_2 greenhouse gases not expected to balance the uptake of carbon by the ocean and emission of carbon from the terrestrial biosphere. These experiments were intended to demonstrate the effect of not reaching or exceeding the balance point for realistic non-CO_2 greenhouse gas forcing. These experiments were identical to the transient emissions experiment until the cessation of carbon emissions. After cessation, non-CO_2 greenhouse gas forcing was held at a constant nonbalancing value, agricultural areas were held constant, and volcanic events and the solar output were fixed to their long-term means. The values chosen were 0.0, 0.95, and 2.0 $W m^{-2}$, respectively. These values are the preindustrial non-CO_2 greenhouse gas forcing, the present-day non-CO_2 greenhouse gas forcing, and the maximum non-CO_2 greenhouse gas forcing projected under RCP 8.5. All values are relative to preindustrial

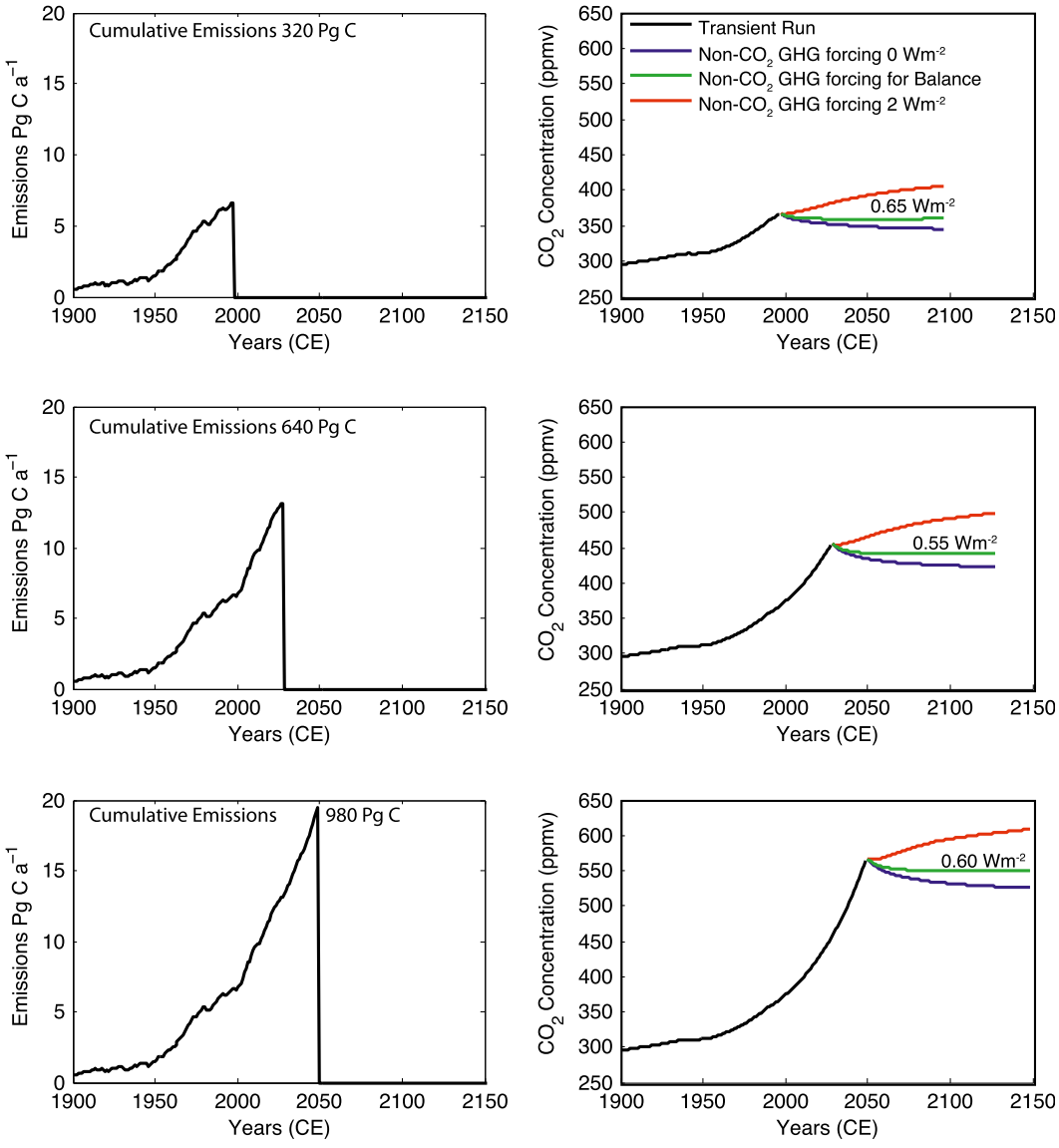

FIG. 1. (left) CO_2 emissions with time and (right) CO_2 concentration with time for three selected cumulative emissions integration points. Atmospheric CO_2 concentrations with time after the cessation of anthropogenic CO_2 emissions given for non-CO_2 greenhouse gas forcings at preindustrial (0.0 W m^{-2}), balancing, and 2.0 W m^{-2} magnitudes.

non-CO_2 greenhouse gas forcing. These experiments are designated as the unbalanced experiments.

3. Results

a. Select results

Selected results for the transient and unbalanced experiments are shown in Fig. 1. The figure displays atmospheric CO_2 concentrations and anthropogenic emissions with time for the preindustrial (0.0 W m^{-2}), balancing, and 2.0 W m^{-2} non-CO_2 radiative forcings. The figure demonstrates the three possible atmospheric CO_2 trajectories after the cessation of anthropogenic CO_2 emissions: atmospheric CO_2 decreases, atmospheric CO_2 remains nearly constant, or atmospheric CO_2 continues to increase without further human CO_2 emissions. For brevity, subsequent figures display only the R_{agg} needed to balance atmospheric carbon verses cumulative carbon emissions. Figure 2 displays the fluxes between and the changes in mass of each of the major carbon pools before and after the cessation of emissions for a selected balance experiment. This figure illustrates the changes in the magnitude of carbon fluxes

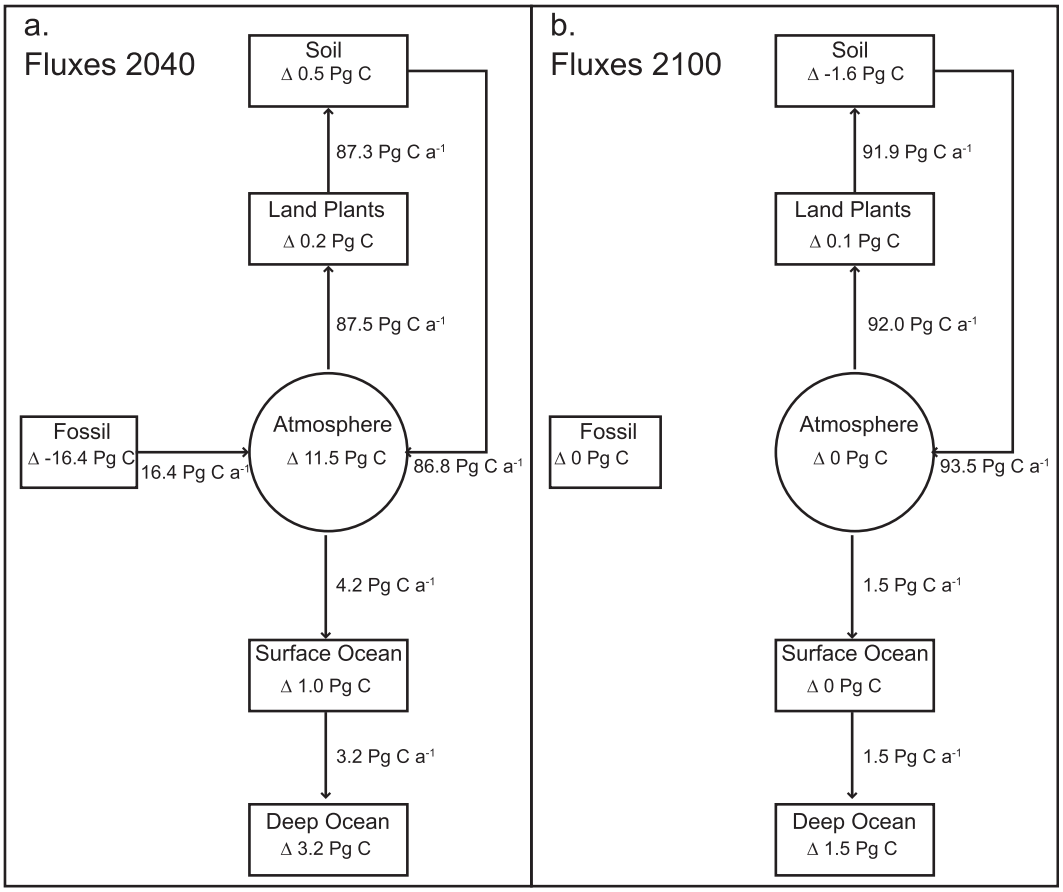

FIG. 2. Net fluxes between and changes in mass of each of the major carbon pools (a) averaged over a decade before the cessation of fossil CO2 emissions and (b) averaged over a decade 50 years after the cessation of fossil CO_2 emissions. Fluxes are from the transient experiment following DEP 8.5, with anthropogenic CO_2 emissions ceasing in the year 2050. The surface ocean is taken at the top 250 m of the water column.

as the earth system transitions to a post–fossil fuel carbon cycle.

b. Balance experiments

Results for the pulse, ramp-up, and transient emissions experiments are shown in Fig. 3. All of the curves have common characteristics, increasing from an R_{agg} of zero (relative to preindustrial times) at a cumulative emission of zero (relative to 1900), reaching a peak R_{agg} (between 160–980 Pg C of cumulative anthropogenic carbon emissions), and declining from this peak with higher cumulative carbon emissions. The highest R_{agg} to induce balance is required for the pulse experiment, and the lowest R_{agg} is required for the ramp-up experiment. This demonstrates that the rate at which carbon is emitted to the atmosphere contributes to the magnitude of R_{agg} needed to balance terrestrial emissions and the ocean uptake of carbon. That is, the balance R_{agg} is path dependent for the time scales considered here.

The transient experiment has a peak balance R_{agg} of $0.65\,W\,m^{-2}$ at 320 Pg C and declines to $0.5\,W\,m^{-2}$ when following the DEP 4.5 and 6.0 emissions trajectories. For the DEP 8.5 trajectory, R_{agg} declines to $0.55\,W\,m^{-2}$ at 640 Pg C then increases again to stabilize at $0.6\,W\,m^{-2}$ for cumulative emissions up to 1920 Pg C. Also shown in Fig. 3c is the historical cumulative anthropogenic carbon emission–non-CO_2 greenhouse gas forcing trajectory. This line shows that the historical magnitude of non-CO_2 greenhouse gas forcing has been above the magnitude needed for CO_2 to continue to increase, if emissions were to cease, since 1900. That is, these model results suggest that Earth has been in the regime of increasing CO_2 without further human CO_2 emissions for most of the industrial age.

The general shape of the curves in Fig. 3 can be explained by the geographic distribution of soil carbon in the UVic ESCM. Figure 4 shows the regions where soil respiration is enhanced by increasing R_{agg} from the preindustrial forcing to the balance forcing for selected

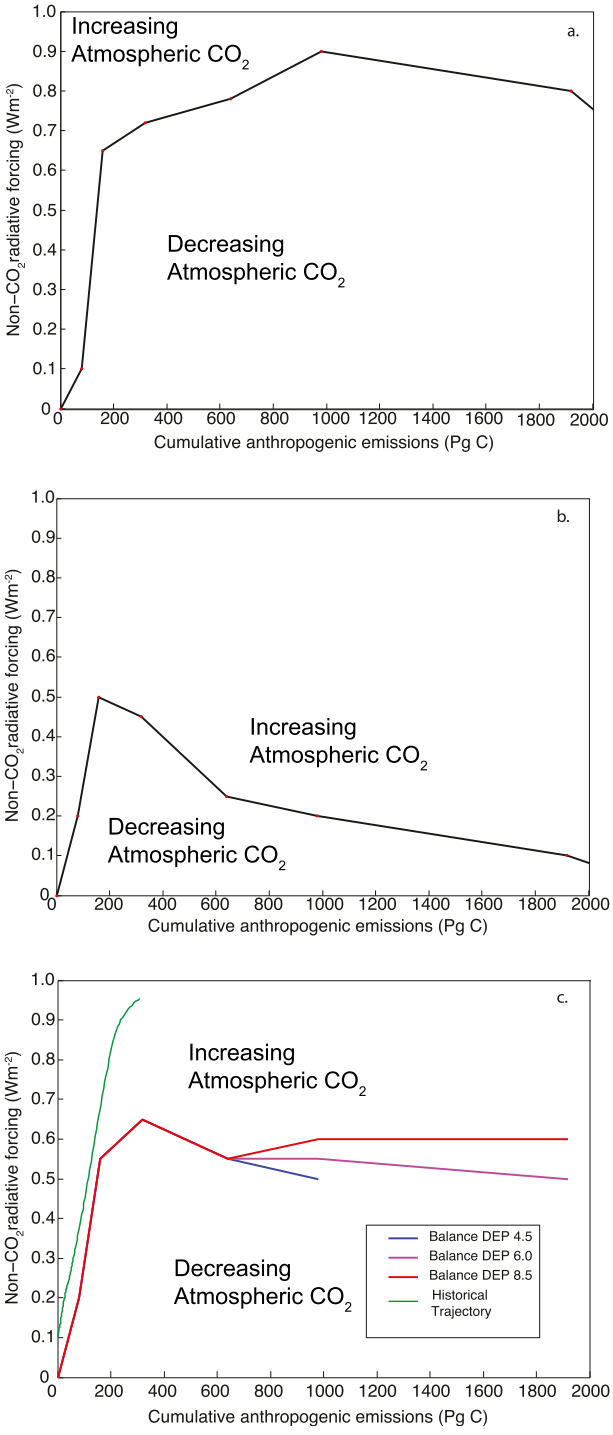

FIG. 3. Non-CO_2 radiative forcing required to maintain a constant level of CO_2 in the atmosphere after the cessation of emissions for a given quantity of cumulative anthropogenic carbon emissions. (a) Carbon emitted as a pulse over the course of 1 year. (b) Carbon emitted at 1% of the cumulative emissions per year for 100 yr. (c) Carbon emitted following a given DEP. The green line shows the historical cumulative anthropogenic carbon emissions–non-CO_2 radiative forcing curve. The current radiative forcing from non-CO_2 greenhouse gases is above the level needed to maintain balance after the cessation of emissions.

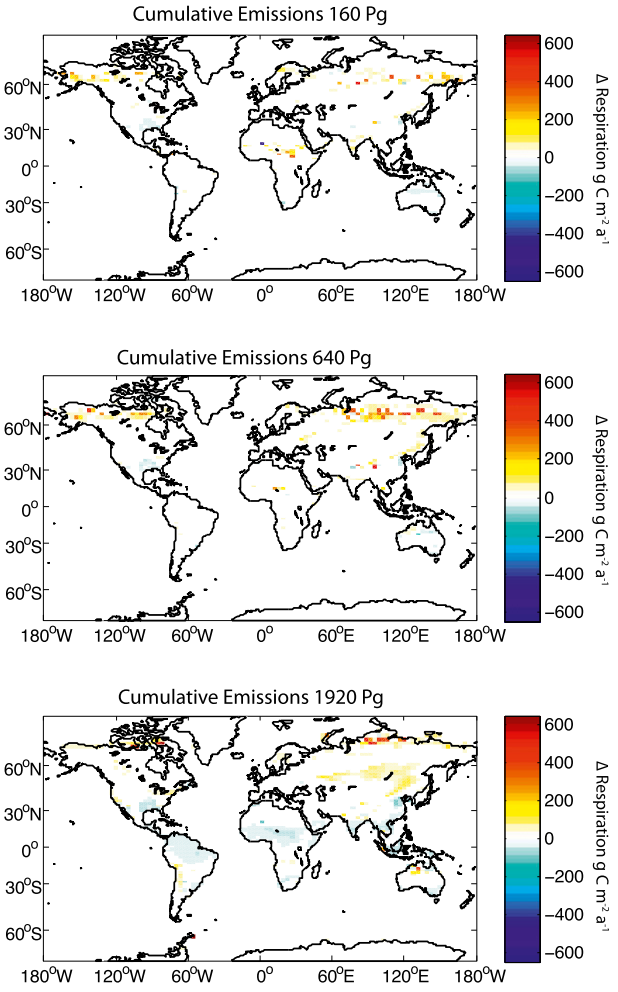

FIG. 4. Difference in soil respiration between model simulation at balancing and preindustrial magnitudes of non-CO_2 greenhouse gas forcing for selected cumulative emission integration points. Maps are for the fifth decade after the cessation of emissions. Notice that in each case most of the additional soil respiration caused by additional non-CO_2 greenhouse gas forcing originates from former permafrost soils. For cumulative emissions of 1920 Pg C, increasing the magnitude of non-CO_2 greenhouse gas forcing reduces the rate of soil respiration in the tropics. This reduction in soil respiration is coincident with a reduction of net primary productivity in these regions. As soil carbon turnover rates are high in the tropics, a reduction in litterfall will quickly lead to a reduction in soil respiration (once litterfall and soil respiration are in equilibrium).

cumulative emission integration points. The excess soil respiration needed to balance ocean uptake is largely derived from regions of decaying permafrost. The large jump in R_{agg} needed to balance ocean uptake between 80 and 160 Pg C is therefore related to the quantity of climate warming needed to destabilize sequestered permafrost carbon.

The inspection of changes in carbon pool sizes for each of the experiments shows that the uptake of carbon

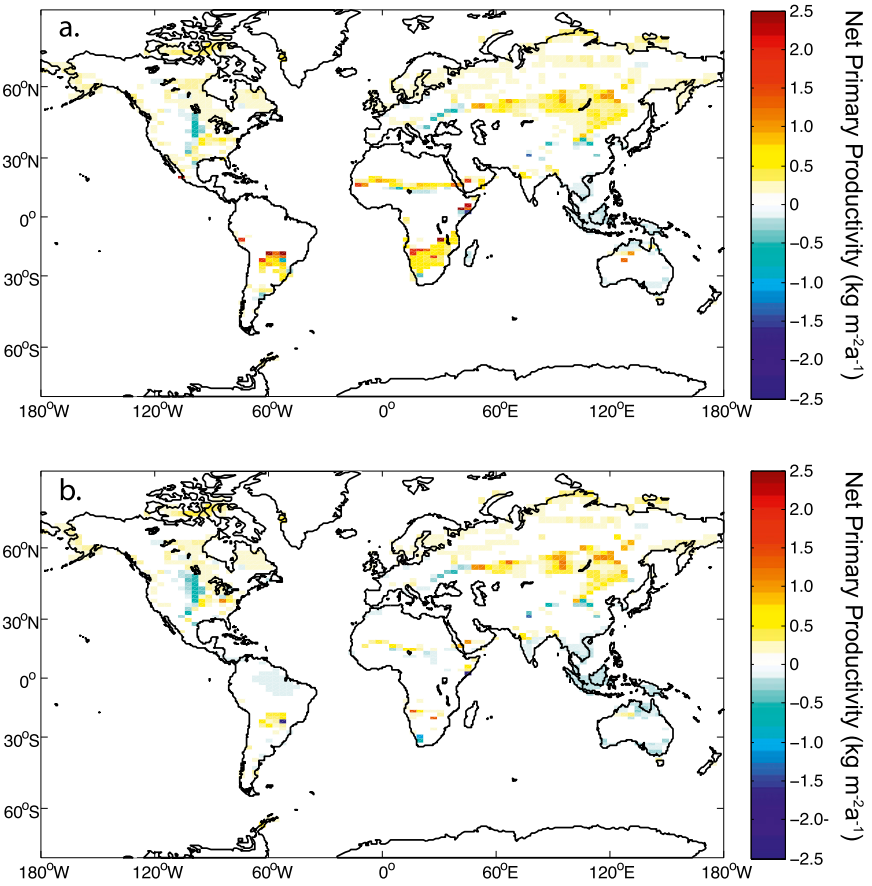

FIG. 5. Difference in NPP between the ramp-up experiment and (a) transient emissions experiment following DEP 8.5 for cumulative anthropogenic carbon emissions of 1920 Pg C (transient emission–ramp-up). (b) As in (a), but following DEP 6.0. Note that positive NPP anomalies are concentrated in central Eurasia, the Sahel, and the subtropics of Africa and South America.

by vegetation makes a significant contribution to carbon uptake in the pulse experiment (15%–40% of ocean uptake) and a negligible contribution in the other experiments. This explains why a higher R_{agg} is needed to induce balance in this experiment than in the other two experiments. In the pulse experiment, enhanced soil respiration must balance the uptake of carbon by both the oceans and terrestrial vegetation. Therefore, a larger R_{agg} is required to further enhance soil respiration.

The difference between the shape of the balance curves in the ramp-up (Fig. 3b) and the transient emissions experiment (Fig. 3c) is curious. Because of the presence of agriculture in the transient emissions experiment, this experiment has higher CO_2 concentrations at the same cumulative anthropogenic (fossil fuel) carbon emissions as the ramp-up experiment. All else being equal, this should shift the curve to the left producing a lower balance R_{agg} for the transient experiments beyond the peak R_{agg} value. The experiments in fact exhibit the opposite behavior. The difference in terrestrial net primary production (NPP) between the ramp-up and transient emissions experiment provides an explanation for the higher balance R_{agg} needed in the transient emissions experiment. For the cumulative anthropogenic carbon emissions integration point of 1920 Pg C, terrestrial NPP at the end of the balanced simulation is 100.4 Pg a^{-1} C for the ramp-up experiment, 113.8 Pg a^{-1} C for transient emissions DEP 8.5 experiment, and 106.7 Pg a^{-1} C for the transient emissions DEP 6.0 experiment. This corresponds to balances in R_{agg} of 0.1, 0.6, and 0.5 W m^{-2}, respectively. Since all of these values of terrestrial NPP are for stable CO_2 concentrations, the higher NPP must be coming from the transition of ecosystems into more carbon intense systems. This negative feedback can be seen in Fig. 5, which maps the difference in terrestrial NPP between the ramp-up and transient emission experiments averaged over the decade beginning 90 years after cumulative

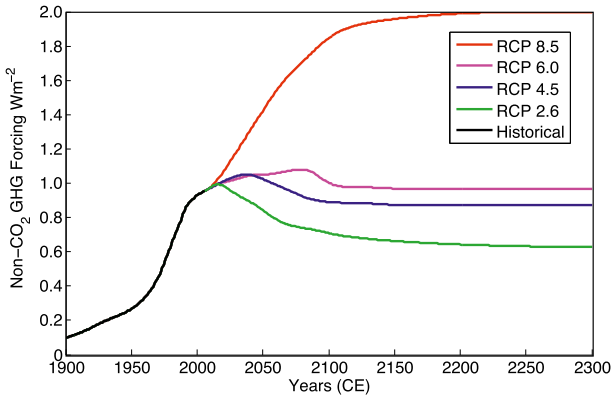

FIG. 6. Estimated radiative forcing from non-CO_2 greenhouse gases for trace gas concentration prescribed for each of the four RCPs (Moss et al. 2010). Note that even the most optimistic estimate for future non-CO_2 greenhouse gas forcing is consistent with approximately balancing the ocean uptake of carbon with emissions from the terrestrial biosphere in the present simulations.

anthropogenic carbon emissions reach 1920 Pg C. The figure shows distinct regions where NPP is higher in the transient emissions experiment than the ramp-up experiment. Specifically, these are in central Eurasia, the Sahel, and the subtropical regions of South America and Africa. These regions are consistent with areas that are pastures in the transient experiment and natural ecosystems in the ramp-up experiment. These pasture regions have a higher NPP than the natural ecosystems they replaced and are associated with a buildup of stored soil carbon in these regions.

Figure 6 shows the estimated non-CO_2 greenhouse gas forcings from trace gas concentrations prescribed for each RCP up to the year 2300. These estimated forcings for year 2300 range from 0.63 W m^{-2} under RCP 2.6 to 2.0 W m^{-2} for RCP 8.5. That is, the estimated non-CO_2 greenhouse gas forcing for the most optimistic RCP is about the same magnitude of radiative forcing needed to balance atmospheric CO_2 in the model experiments conducted here.

c. *Unbalanced experiments*

Results of the unbalanced experiments are shown in Tables 1, 2, and 3. Under a continued modern R_{agg} of 0.95 W m^{-2}, the atmospheric CO_2 concentration increases an additional 11–22 ppmv before peaking in the twenty-third or twenty-fourth century (Table 1). That is, CO_2 continues to build up very slowly in the atmosphere for hundreds of years after anthropogenic carbon emissions cease. The actual amount of carbon released by soils is substantial (167–400 Pg C), but most of this carbon is absorbed by the oceans (68%–89%; Table 2). Almost as much carbon is absorbed by land plants as builds up in the atmosphere. Under an R_{agg} commensurate to that in RCP 8.5 (2.0 W m^{-2}), soils release more carbon (400–570 Pg C), and the atmosphere takes up a larger fraction of this carbon (27%–35%), but the oceans continue to take up the largest share of carbon (56%–64%; Table 3). The additional increase in CO_2 concentration is 64–86 ppmv, but the effects of this increase in CO_2 are minor compared to that of imposing an unbalanced radiative forcing of 2.0 W m^{-2} on the Earth system. These results suggest that the consequences of being beyond the carbon cycle balance point are mild for non-CO_2 greenhouse gas concentration observed in the contemporary atmosphere. After the cessation of anthropogenic carbon emissions, atmospheric CO_2 will continue to build up in the atmosphere but at a rate that is an order of magnitude slower than during the fossil fuel era.

TABLE 1. Peak CO_2 concentrations for a given quantity of cumulative anthropogenic carbon emissions, year of peak, and change in concentration relative to 20 years after shutdown.

Cumulative emissions (Pg C)	Year of peak (CE)	Peak CO_2 (ppmv)	Δ CO_2 (ppmv)
Unbalanced 0.95 W m^{-2}			
80	2321	327	17
160	2360	342	15
320	2366	379	16
640	2241	460	12
980	2213	569	11
1920	2244	949	22
Unbalanced 2.0 W m^{-2}			
160	2436	394	66
320	2347	431	64
640	2422	521	67
980	2341	639	70
1920	2249	1020	86

d. *Breakdown of assumptions*

Not all of the attempts to find a carbon cycle balance point were successful. Figure 7 displays an attempt to balance at an integration point of 3840 Pg C for the transient emissions experiment following DEP 8.5. At the time anthropogenic CO_2 emissions cease, in this simulation carbon emissions from the terrestrial biosphere are already larger than the ability of the oceans to absorb carbon. The terrestrial emissions soon fall off as the soil carbon pool is depleted (dropping 394 Pg C) and a strong afforestation feedback takes hold (adding 46 Pg C to land plants). Having exhausted the pool of soil carbon available for decay, terrestrial carbon emission becomes smaller than the ocean uptake of CO_2, and atmospheric CO_2 concentration begins to decline. For this quantity of cumulative anthropogenic emissions, no constant level of non-CO_2 greenhouse gas forcing after the cessation of emissions will produce a cancellation of terrestrial emissions and the ocean uptake of carbon.

TABLE 2. Cumulative emissions from soils from the year of the cessation of anthropogenic carbon emissions to year of peak atmospheric CO_2. Also shown is the partition of this carbon to the atmosphere, land plants, and the oceans.

Cumulative emissions (Pg C)	Year of peak (CE)	Soil pool (Pg C)	Atmosphere pool (Pg C)	Land plants pool (Pg C)	Ocean pool (Pg C)
		Unbalanced 0.95 W m^{-2}			
160	2360	−166.8	29.7	5.6	113.9
320	2366	−227.8	25.9	16.7	169.8
640	2241	−240.3	11.4	18.6	203.3
980	2213	−259.3	4.3	19.8	230.2
1920	2244	−401.0	33.6	38.6	320.9
		Unbalanced 2.0 W m^{-2}			
160	2436	−398.7	138.9	25.2	225.2
320	2347	−407.8	135.2	23.7	247.7
640	2422	−524.6	139.8	46.6	331.9
980	2341	−565.0	152.8	44.6	363.4
1920	2249	−569.5	183.9	27.5	355.6

4. Discussion

a. Why is balancing atmospheric CO_2 possible?

A priori there is no reason to suspect the net emissions of CO_2 from the terrestrial land surface will balance the uptake of carbon by the oceans after the cessation of anthropogenic CO_2 emissions. That this phenomenon does occur within the UVic ESCM for multiple cumulative carbon emissions and emissions trajectories begs for a simple mechanistic explanation. In this section, a rudimentary description of the ocean uptake of carbon and soil respiration will be invoked to argue that the functional form of the two processes, in addition to coincidences in the rate constants and carbon pool sizes of soil carbon and the surface ocean, are what allow for balancing atmospheric CO_2.

As outlined in the introduction, the flux of carbon into the surface ocean is proportional to the difference in CO_2 partial pressure between the atmosphere and the ocean. For a given location in the ocean, this relationship can be described by

$$\frac{\partial \mathrm{DIC}}{\partial t} = \frac{k_w}{z_{\mathrm{ml}}}([\mathrm{CO_2}]_{\mathrm{sat}} - [\mathrm{CO_2}]_w), \qquad (2)$$

where DIC is dissolved inorganic carbon, k_w is the piston velocity, z_{ml} is the thickness of the mixed layer, $[\mathrm{CO_2}]_{\mathrm{sat}}$ is the aqueous concentration of CO_2 at which the surface ocean would be in chemical equilibrium with the atmosphere, and $[\mathrm{CO_2}]_w$ is the instantaneous concentration of CO_2 in ocean water (e.g., Najjar 1992). The terms on right hand side are in turn functions of time, ocean stratification, ocean temperature, and other variables. The term $[\mathrm{CO_2}]_w$ in particular is affected by the reaction of CO_2 with water and solutes into other species of DIC and by marine organisms producing and consuming CO_2. Considering typical piston velocities [which vary an order of magnitude as a function of surface wind speed and other variables (e.g., Najjar 1992)] and a typical mixed layer depth for the ocean, the rate constant of this relationship is in the order of 1–10 $\times$ 10^{-7} s^{-1} (e.g., Najjar 1992). Recalling that only about 1 part in 200 of DIC is held as CO_{2aq} due to the carbonate buffering system of the ocean, this rate constant reduces to 1–10 $\times$ 10^{-9} s^{-1} (e.g., Najjar 1992).

Once carbon enters the surface ocean, the biological pump and subduction of surface waters transport a portion of this carbon into the ocean interior (e.g., Greenblatt and Sarmiento 2004). Upwelling water from the deep ocean will partially compensate for this sink for carbon; however, due to the slow rate of the ocean overturning transport of carbon into the deep ocean, the ocean is expected to remain a sink of carbon for millennia (e.g., Eby

TABLE 3. Fractional uptake by the atmosphere, land plants, and the oceans of carbon emitted by soils between the cessation of anthropogenic carbon emissions and peak atmospheric CO_2 concentration.

Cumulative emissions (Pg C)	Year of peak (CE)	Atmosphere pool (%)	Land plants pool (%)	Ocean pool (%)
		Unbalanced 0.95 W m^{-2}		
160	2360	18	14	68
320	2366	11	14	75
640	2241	5	10	85
980	2213	2	9	89
1920	2244	8	12	80
		Unbalanced 2.0 W m^{-2}		
160	2436	35	9	56
320	2347	33	6	61
640	2422	27	10	63
980	2341	27	9	64
1920	2249	32	6	62

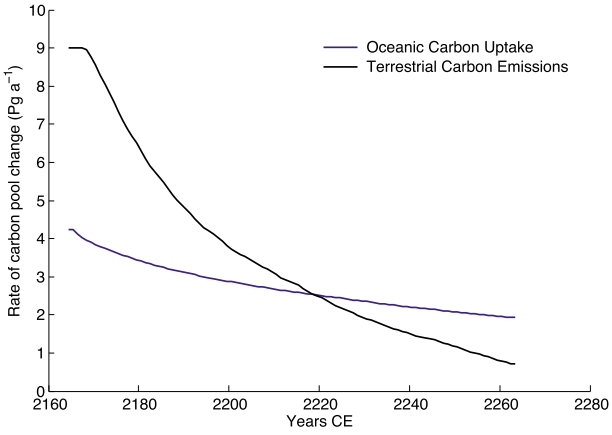

FIG. 7. Rate of the ocean uptake of carbon and terrestrial emissions of carbon for a simulation where the rates cannot be balanced. Opposite sign conventions are used for the two carbon fluxes to accommodate comparison of the magnitude of each. Notice that terrestrial emissions are already larger than the ocean uptake when emissions cease. This example is from the transient emissions experiment for 3840 Pg of cumulative anthropogenic carbon emissions with a non-CO_2 radiative forcing of 3.0 W m^{-2} after the cessation of carbon emissions.

et al. 2009). The strength of the deep ocean carbon sink is dependent on the strength of the biological pump, the concentration of surface water DIC at the deep-water formation sites, the rate of meridional overturning circulation, and the concentration of DIC in water upwelling from the ocean interior (e.g., Greenblatt and Sarmiento 2004). If these factors were to remain constant in time, then after an initial exponential decrease (as the surface ocean equilibrates with the atmosphere) the ocean uptake of carbon should asymptotically approach this background deep ocean uptake rate. However, it is a robust finding of ocean general circulation model simulations that the rate of meridional overturning circulation (MOC) is expected to decline in the first centuries of climate warming (Weaver et al. 2012), which implies that the ocean uptake of carbon should decline in tandem with the slowing of the MOC.

The surface ocean holds approximately 700 Pg of dissolved inorganic carbon under contemporary conditions (Falkowski et al. 2000). If the solubility and carbonate chemistry of CO_2 were held constant, the surface ocean could hold another 700 Pg C for a doubling of atmospheric CO_2. However, the effects of CO_2 on solubility, carbonate chemistry, and ocean dynamics reduce this total to approximately 350–600 Pg C for a doubling of atmospheric CO_2, when simulated by ocean biogeochemical models (Greenblatt and Sarmiento 2004). The surface ocean will absorb much of this total during a transient increase in atmospheric CO_2. Therefore, when anthropogenic CO_2 emissions cease, the difference between the quantity of carbon the surface ocean has and the quantity of carbon the surface ocean needs (to be in equilibrium with the atmosphere) will be smaller. Once deep ocean processes dominate the ocean uptake of carbon, the surface ocean is left with a perpetual deficit in the quantity of carbon needed to achieve equilibrium with the atmosphere.

The loss of carbon from soils occurs if soil respiration exceeds the rate of litterfall into soils (Davidson and Janssens 2006). As soil respiration is a function of soil temperature, many models show this transition occurring in the late twenty-first or twenty-second century as the climate warms (Davidson and Janssens 2006). In nonpermafrost soils, approximately 100–200 Pg C of soil carbon are estimated to be vulnerable to net soil respiration. Permafrost-affected soils contain 1700 Pg C, about 800 Pg C of which is sequestered in frozen soils in the top 3 m of the soil column (Tarnocai et al. 2009). Together, the terrestrial land surface has a total of approximately 900 to 1000 Pg C vulnerable to decay (but the quantity that actually becomes available to decay is dependent on the magnitude of surface temperature increase). The rate of soil respiration has been shown to be proportional to the quantity of soil carbon available for decay such that, given a pulse of soil carbon, the quantity of carbon will be reduced asymptotically toward zero (Luo and Zhou 2006). The rate constant for soil respiration for ideal moisture and temperature conditions varies by the chemical makeup of the organic matter available for decay and the microbial community conducting the decomposition. This rate constant has been measured to be between 1–10 $\times$ 10^{-9} s^{-1} for typical mixtures of organic materials in soils (Luo and Zhou 2006). The cold temperatures of former permafrost soils imply that effective rates constants for these soils are in the slow end of the range (e.g., Dutta et al. 2006). Results from MacDougall et al. (2012) show that the UVic ESCM simulates a roughly linear release of sequestered permafrost carbon into an active soil carbon pool for changes in surface temperature between 1° and 5°C (see Fig. 8). For a doubling of CO_2 (an approximately 3°C temperature increase), the results from MacDougall et al. (2012) show an approximately 400 Pg release of carbon to active soils from the permafrost.

From these considerations, one can see why it is possible to balance the carbon cycle within the UVic ESCM for the century after the cessation of carbon emissions. The phenomenon is conditional on the functional form of each process, rate constants, and the quantity of carbon available for decay verses the quantity of carbon that the surface ocean requires to be in equilibrium with the atmosphere. Soil respiration has a negative exponential functional form, which after an initial period of

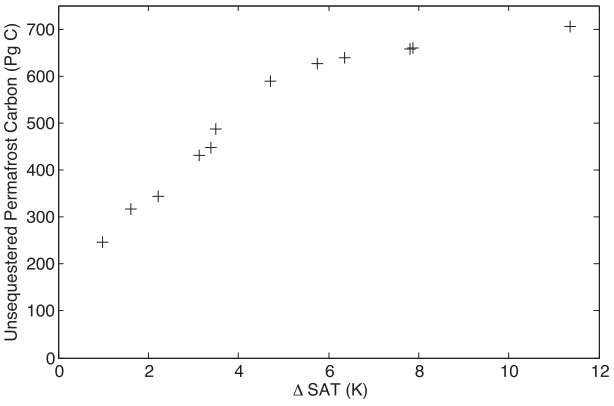

FIG. 8. Change in surface air temperature (SAT) vs the release of carbon from the permafrost carbon pool to the active soil carbon pool, as simulated by the UVic ESCM for year 2300 following four emissions pathways (MacDougall et al. 2012). Note that between temperature increases of between 1° and 5°C, the release of carbon from its sequestered state is nearly linear.

rapid decline can be approximated as a linearly declining emissions rate. Ocean uptake takes on a linear declining functional form once the transport of carbon into the deep ocean becomes the dominant process (due to the slowing of meridional overturning circulation). Coincidentally, the rate constants of the uptake of carbon into the surface ocean and heterotrophic soil respiration are similar (larger for the ocean than land). In addition, the quantity of carbon available for decay in the terrestrial land surface and the surface ocean's deficit in carbon are of a similar magnitude (larger for the land than the ocean). By manipulating non-CO_2 greenhouse gas forcing, one changes the rate of soil respiration (temperature dependent), controls how much carbon is liberated from permafrost carbon, and changes the partial pressure of CO_2 in ocean water (pulling the total ocean uptake of carbon and liberated permafrost carbon in opposite directions). These factors, by coincidence, happen to be close enough in value that manipulating non-CO_2 greenhouse gas forcing can generate an approximate balance between the net emission of carbon from the terrestrial biosphere and the uptake of carbon by the oceans for over a century.

b. Model dependence

The results presented here are model dependent. The Coupled Carbon Cycle Model Intercomparison Project (C^4MIP) showed that carbon cycle models have a range of simulated ocean uptake of carbon (between 4 and 10 Pg a^{-1} C at 2100) and have varying responses from the terrestrial biosphere (Friedlingstein et al. 2006). If these types of balance experiments are conducted with other carbon cycle models, different magnitudes of non-CO_2 greenhouse gas forcing, required to induce balance, would be expected. As discussed above, the ability to balance the atmospheric carbon depends on several quantities within the earth system being of coincident magnitude and functional form. Other Earth system models may simulate contrasting behavior from the global carbon cycle.

The cloud, water vapor, albedo, and trace gas feedbacks that determine planetary climate sensitivity have a similar effect as non-CO_2 greenhouse gases (warming the surface while not increasing the ability of the ocean to absorb carbon). It is therefore expected that variations in climate sensitivity between models will also change the quantity of non-CO_2 greenhouse gases needed to balance atmospheric CO_2. Low climate sensitivity models are expected to require more non-CO_2 greenhouse gas forcing to induce continued post–fossil fuel buildup of atmospheric CO_2 than models with a higher climate sensitivity.

c. Time scale of balance

The model experiments conducted here consider the time period up to 400 years after the cessation of anthropogenic CO_2 emissions. The behavior of the model at longer time scales is expected to be different. Balancing the atmospheric carbon pool requires that the quantity of carbon vulnerable for decay in soils be of the same order of magnitude as the quantity of carbon that the surface ocean requires to be in equilibrium with the atmosphere. However, the capacity of the full ocean to absorb carbon is immense (e.g., Falkowski et al. 2000), and the surface ocean deficit in carbon will exist long after the vulnerable pool of carbon has been depleted. At millennial time scales it is expected that the permafrost carbon version of the UVic ESCM will behave much as earlier versions of the model (Eby et al. 2009) with the additional liberated permafrost carbon by simply adding to the total anthropogenic carbon pulses.

d. Policy implications

Article 2 of the United Nations framework convention on climate change commits its signatories to the "stabilization of greenhouse gas concentrations in the atmosphere at a level that would prevent dangerous anthropogenic interference with the climate system." The results presented here indicate that sharp reductions in the concentration of non-CO_2 greenhouse gases may be required to prevent CO_2 from continuing to build up in the atmosphere (albeit slowly). That said, stabilizing atmospheric greenhouse gas concentrations may not be sufficient to prevent "dangerous anthropogenic interference with the climate system." Achieving that goal may require the removal of greenhouse gases from the atmosphere (e.g., Hansen et al. 2008). It is

possible that enhanced natural sources of biogenic methane, irreversible damage to the caping formations of geological methane, and/or slow destabilization of methane clathrates could replace the current anthropogenic sources of methane (O'Connor et al. 2010). This could keep non-CO_2 greenhouse gas concentrations above the quantity needed to stabilize atmospheric CO_2, even if anthropogenic sources of these gases are eliminated.

e. Forcing and feedback uncertainties

The sudden cessation of anthropogenic CO_2 emissions is an implausible future emissions trajectory, and the model experiments conducted here are intended to be sensitivity experiments. However, if such an event were to occur, uncertainties in the behavior of several Earth system processes would affect whether atmospheric CO_2 concentration would continue to increase. The present-day radiative forcing from anthropogenic aerosols is subject to considerable uncertainty (Murphy et al. 2009). The magnitude of this forcing and the forcing from non-CO_2 greenhouse gases will determine the net change in radiative forcing upon the cessation of aerosol emissions. The strength of the climate feedbacks that determine planetary climate sensitivity is also expected to strongly affect the rate at which carbon is released from permafrost soils (MacDougall et al. 2012). Balancing the atmospheric carbon pool is contingent on the existence of a vulnerable source of carbon within the terrestrial land surface (permafrost carbon) to counteract the uptake of carbon by the oceans. Both the size and vulnerability of the permafrost carbon pool are subject to considerable uncertainties (Schuur and Abbottand 2011). All of these uncertainties will affect the magnitude of non-CO_2 greenhouse gas forcing required to induce a near balance in the atmospheric carbon pool.

5. Conclusions

Here, we sought to answer the question "if anthropogenic CO_2 emissions cease, will atmospheric CO_2 concentration continue to increase?" Our experiments show that for cumulative anthropogenic carbon emissions up to about 2000 Pg C, there is a magnitude of non-CO_2 greenhouse gas forcing that will create a balance between emissions from the terrestrial biosphere and the uptake of carbon by the oceans. If non-CO_2 greenhouse gases are maintained above this magnitude, then CO_2 will continue to build up in the atmosphere for centuries after the cessation of anthropogenic CO_2 emissions. If non-CO_2 greenhouse gases are below this magnitude, then atmospheric concentrations of CO_2 will decline after the cessation of emissions. That simulated Earth is so close to the crossover between decreasing and increasing atmospheric CO_2 appears to be a coincidence created by similar magnitudes in the quantity of carbon that could be liberated from permafrost soils and the quantity of carbon that the surface ocean requires to be in equilibrium with the atmosphere.

The magnitude of non-CO_2 greenhouse gas forcing required to balance atmospheric CO_2 is a function of how much carbon has been emitted to the atmosphere and the rate at which it has been emitted. The historical trajectory of non-CO_2 greenhouse gas forcing has been above the simulated balancing magnitude since 1900. That is, if anthropogenic emissions were to cease tomorrow, the UVic ESCM projects that CO_2 would continue to build up in the atmosphere. However, the consequences of being in the regime of increasing CO_2 concentrations after the cessation of anthropogenic emissions are relatively mild. If current non-CO_2 greenhouse gas forcing is maintained indefinitely, our admittedly model-dependent results suggest that we might expect an 11–22 ppmv increase in CO_2 after human emissions cease.

Acknowledgments. The authors are grateful to NSERC for support in the form of a CGS scholarship for AHMD and a Discovery Grant awarded to AJW. We thank C. Goldblatt for critical comments on an early draft of this manuscript. We thank M. Hain and H. D. Matthews for their useful comments.

REFERENCES

Archer, D., 1996: A data-driven model of the global calcite lysocline. *Global Biogeochem. Cycles,* **10,** 511–526.

Avis, C. A., 2012: Simulating the present-day and future distribution of permafrost in the UVic Earth System Climate Model. Ph.D. dissertation, University of Victoria, 274 pp.

——, A. J. Weaver, and K. J. Meissner, 2011: Reduction in areal extent of high-latitude wetlands in response to permafrost thaw. *Nat. Geosci.,* **4,** 444–448, doi:10.1038/ngeo1160.

Baldocchi, D., and R. Valentini, 2004: Geographic and temporal variation of carbon exchange by ecosystems and their sensitivity to environmental perturbations. *The Global Carbon Cycle,* C. B. Field and M. R. Raupach, Eds., Island Press, 295–316.

Davidson, E., and I. Janssens, 2006: Temperature sensitivity of soil carbon decomposition and feedbacks to climate change. *Nature,* **440,** 165–173.

Denman, K., and Coauthors, 2007: Couplings between changes in the climate system and biogeochemistry. *Climate Change 2007: The Physical Science Basis,* S. Solomon et al., Eds., Cambridge University Press, 499–587.

Dutta, K., E. A. G. Schuur, J. C. Neff, and S. A. Zimov, 2006: Potential carbon release from permafrost soils of northeastern Siberia. *Global Change Biol.,* **12,** 2336–2351.

Eby, M., K. Zickfeld, A. Montenegro, D. Archer, K. J. Meissner, and A. J. Weaver, 2009: Lifetime of anthropogenic climate change: Millennial time scales of potential CO_2 and surface temperature perturbations. *J. Climate,* **22,** 2501–2511.

Falkowski, P., and Coauthors, 2000: The global carbon cycle: A test of our knowledge of Earth as a system. *Science,* **290,** 291–296.

Forster, P., and Coauthors, 2007: Changes in atmospheric constituents and in radiative forcing. *Climate Change 2007: The Physical Science Basis,* S. Solomon et al., Eds., Cambridge University Press, 129–234.

Friedlingstein, P., and Coauthors, 2006: Climate–carbon cycle feedback analysis: Results from the C^4MIP model intercomparison. *J. Climate,* **19,** 3337–3353.

Gillett, N., V. Arora, K. Zickfeld, S. Marshall, and W. Merryfield, 2011: Ongoing climate change following a complete cessation of carbon dioxide emissions. *Nat. Geosci.,* **4,** 83–87.

Greenblatt, J. B., and J. L. Sarmiento, 2004: Variability and climate feedback mechanisms in ocean uptake of CO_2. *The Global Carbon Cycle,* C. B. Field and M. R. Raupach, Eds., Island Press, 257–278.

Hansen, J., and Coauthors, 2008: Target atmospheric CO_2: Where should humanity aim? *Open Atmos. Sci. J.,* **2,** 217–231.

Huntingford, C., P. Cox, L. Mercado, S. Sitch, N. Bellouin, O. Boucher, and N. Gedney, 2011: Highly contrasting effects of different climate forcing agents on terrestrial ecosystem services. *Philos. Trans. Roy. Soc.,* **A369,** 2026–2037.

Jenkinson, D., D. Adams, and A. Wild, 1991: Model estimates of CO_2 emissions from soil in response to global warming. *Nature,* **351,** 304–306.

Le Qéré, C., and N. Metzl, 2004: Natural processes regulating the ocean uptake of CO_2. *The Global Carbon Cycle,* C. B. Field and M. R. Raupach, Eds., Island Press, 243–256.

Lohmann, U., and J. Feichter, 2005: Global indirect aerosol effects: A review. *Atmos. Chem. Phys.,* **5,** 715–737.

Luo, Y., and X. Zhou, 2006: *Soil Respiration and the Environment.* Academic Press, 328 pp.

MacDougall, A. H., C. A. Avis, and A. J. Weaver, 2012: Significant contribution to climate warming from permafrost carbon feedback. *Nat. Geosci.,* **5,** 719–721, doi:10.1038/NGEO1573.

Malhi, Y., and Coauthors, 2009: Exploring the likelihood and mechanism of a climate-change-induced dieback of the Amazon rainforest. *Proc. Natl. Acad. Sci. USA,* **106,** 20 610–20 615.

Matthews, H. D., and A. Weaver, 2010: Committed climate warming. *Nat. Geosci.,* **3,** 142–143.

——, and K. Zickfeld, 2012: Climate response to zeroed emissions of greenhouse gases and aerosols. *Nat. Climate Change,* **2,** 338–341.

——, A. J. Weaver, K. J. Meissner, N. P. Gillett, and M. Eby, 2004: Natural and anthropogenic climate change: Incorporating historical land cover change, vegetation dynamics and the global carbon cycle. *Climate Dyn.,* **22,** 461–479, doi:10.1007/s00382-004-0392-2.

Meissner, K. J., A. J. Weaver, H. D. Matthews, and P. M. Cox, 2003: The role of land–surface dynamics in glacial inception: A study with the UVic Earth System Model. *Climate Dyn.,* **21,** 515–537.

Moss, R. H., and Coauthors, 2010: The next generation of scenarios for climate change research and assessment. *Nature,* **463,** 747–754, doi:10.1038/nature08823.

Murphy, D., S. Solomon, R. Portmann, K. Rosenlof, P. Forster, and T. Wong, 2009: An observationally based energy balance for the earth since 1950. *J. Geophys. Res.,* **114,** D17107, doi:10.1029/2009JD012105.

Najjar, R. G., 1992: Marine biogeochemistry. *Climate System Modeling,* K. E. Trenberth, Ed., Cambridge University Press, 241–282.

O'Connor, F. M., and Coauthors, 2010: Possible role of wetlands, permafrost, and methane hydrates in the methane cycle under future climate change: A review. *Rev. Geophys.,* **48,** RG4005, doi:10.1029/2010RG000326.

Schmittner, A., A. Oschlies, H. D. Matthews, and E. D. Galbraith, 2008: Future changes in climate, ocean circulation, ecosystems, and biogeochemical cycling simulated for a business-as-usual CO_2 emission scenario until year 4000 AD. *Global Biogeochem. Cycles,* **22,** GB1013, doi:10.1029/2007GB002953.

Scholes, R., and E. B. de Colstoun, cited 2012: ISLSCP II global gridded soil characteristics. ORNL Distributed Active Archive Center dataset. [Available online at http://daac.ornl.gov/ISLSCP_II/guides/islscp2_soils_1deg.html.]

Schuur, E. A. G., and B. Abbott, 2011: Climate change: High risk of permafrost thaw. *Nature,* **480,** 32–33.

——, and Coauthors, 2008: Vulnerability of permafrost carbon to climate change: Implications for the global carbon cycle. *Bioscience,* **58,** 701–714.

Sigman, D. M., M. P. Hain, and G. H. Haug, 2010: The polar ocean and glacial cycles in atmospheric CO_2 concentration. *Nature,* **466,** 47–55, doi:10.1038/nature09149.

Tarnocai, C., J. G. Canadell, E. A. G. Schuur, P. Kuhry, G. Mazhitova, and S. Zimov, 2009: Soil organic carbon pools in the northern circumpolar permafrost region. *Global Biogeochem. Cycles,* **23,** GB2023, doi:10.1029/2008GB003327.

Weaver, A. J., and Coauthors, 2001: The UVic Earth System Climate Model: Model description, climatology, and applications to past, present and future climates. *Atmos.–Ocean,* **39,** 361–428.

——, and Coauthors, 2012: Stability of the Atlantic meridional overturning circulation: A model intercomparison. *Geophys. Res. Lett.,* **39,** L20709, doi:10.1029/2012GL053763.